

# Sub-linear radiation power dependence of photo-excited resistance oscillations in two-dimensional electron systems

Jesús Iñarrea,<sup>1,2</sup> R. G. Mani,<sup>3</sup> and W. Wegscheider<sup>4,5</sup>

<sup>1</sup>*Escuela Politécnica Superior, Universidad Carlos III, Leganes, Madrid, 28911, Spain*

<sup>2</sup>*Unidad Asociada al Instituto de Ciencia de Materiales, CSIC, Cantoblanco, Madrid, 28049, Spain.*

<sup>3</sup>*Department of Physics and Astronomy, Georgia State University, Atlanta, GA 30303 U.S.A.*

<sup>4</sup>*Universität Regensburg, 93053 Regensburg, Germany*

<sup>5</sup>*Laboratorium für Festkörperphysik, ETH-Zürich, 8093 Zürich, Switzerland*

(Dated: November 5, 2018)

We find that the amplitude of the  $R_{xx}$  radiation-induced magnetoresistance oscillations in GaAs/AlGaAs system grows nonlinearly as  $A \propto P^\alpha$  where  $A$  is the amplitude and the exponent  $\alpha < 1$ . This striking result can be explained with the radiation-driven electron orbits model, which suggests that the amplitude of resistance oscillations depends linearly on the radiation electric field, and therefore on the square root of the power,  $P$ . We also study how this sub-linear power law varies with lattice temperature and radiation frequency.

PACS numbers: 73.40.-c, 73.43.Qt, 73.43.-f, 73.21.-b

## I. INTRODUCTION

Superconductivity[1] and quantum Hall effects[2, 3] are known to present two distinct and interesting examples of zero-resistance states in material systems. Another interesting example occurs in the quantum Hall two-dimensional electron system (2DES) when the 2DES is irradiated with microwave and terahertz band radiation in the presence of a transverse magnetic field. Here, it becomes possible to photo-excite into zero-resistance states in this low dimensional system.[4, 5] Photo-excited transport in the 2DES has become a topic of experimental and theoretical interest since this observation.[4–44] Periodic in  $B^{-1}$  radiation-induced magnetoresistance oscillations, which lead into the radiation-induced zero-resistance states, are now understood to be a consequence of radiation-frequency ( $f$ ) and magnetic field ( $B$ ) dependent, scattering at impurities [24–28] and/or a change in the distribution function[6, 31, 38]. And, vanishing resistance at the oscillatory minima is explained as a feature of negative resistance instability and current domain formation.[25, 34, 42] In spite of the progress, there remain many aspects that could be better understood from including, for example, the growth of the oscillatory effect vs. the radiation intensity,  $P$ . Here, a number of works have numerically evaluated the radiation-induced magnetoresistance oscillations for several  $P$  and graphically presented the results,[24, 32, 35] while Dmitriev et al.,[31] have suggested that the correction to the dark dc conductivity is linear in  $P$ . [31] A comparison of experiment with theory, so far as the  $P$ -dependence is concerned, could help to identify the importance of the invoked mechanisms in these theories.[36]

Thus, we examine the growth of the radiation-induced magneto-resistance oscillations with  $P$ . Experiment indicates that the amplitude  $A$  of the radiation-induced oscillatory diagonal resistance ( $R_{xx}$ ), grows nonlinearly

with  $P$  and can be described by  $A \propto P^\alpha$  where the exponent  $\alpha < 1$ . At the same time, according to experiment,  $\alpha$  also depends on the lattice temperature  $T$  and radiation frequency  $f$ . Since such non-linear growth of  $A$  with  $P$ ,  $T$ , and  $f$  had not been predicted, we propose a theoretical explanation. The explanation utilizes the *radiation-driven electron orbit model*, [32] where radiation forces the orbit center of the Landau states to move back and forth in the direction of the radiation electric field at the frequency of radiation, and the  $R_{xx}$  oscillations reflect the periodic motion of the electron orbits center. This theory establishes that the amplitude ( $A_{Lan}$ ) of the orbit center motion, sets the amplitude  $A$  of the  $R_{xx}$  oscillations, and that  $A_{Lan}$  is proportional to the radiation electric field. Since the radiation power  $P$  is proportional to the square of the radiation electric field, it follows that  $R_{xx}$  and  $A$  will depend on the square root of  $P$ , at the lowest temperatures. The experiments indicate that  $\alpha$  is close to 0.5 at lower temperatures.

## II. THEORETICAL MODEL

The above mentioned theory[32, 33, 39] was proposed to explain the  $R_{xx}$  of an irradiated 2DES at low  $B$ . We obtained the exact solution of the corresponding electronic wave function[32, 39, 45–48]:

$$\Psi(x, t) \propto \phi_n(x - X - x_{cl}(t), t) \quad (1)$$

, where  $\phi_n$  is the solution for the Schrödinger equation of the unforced quantum harmonic oscillator,  $X$  is the center of the orbit for the electron motion,  $x_{cl}(t)$  is the classical solution of a forced harmonic oscillator:

$$\begin{aligned} x_{cl} &= \frac{eE_o}{m^* \sqrt{(w_c^2 - w^2)^2 + \gamma^4}} \cos wt \\ &= A_{Lan} \cos wt \end{aligned} \quad (2)$$

where  $e$  is the electron charge,  $\gamma$  is a phenomenologically-introduced damping factor for the electronic interaction with acoustic phonons,  $w_c$  the cyclotron frequency,  $E_0$  the radiation electric field. Then, the obtained wave function is the same as the standard harmonic oscillator where the center is displaced by  $x_{cl}(t)$ . Thus, the orbit centers are not fixed, but they oscillate harmonically at the radiation field frequency  $w = 2\pi f$ . Then, by this micro(MW)-driven periodic motion, electrons in their orbits (quantum oscillators) interact with the lattice ions being damped and emitting acoustic phonons. In the  $x_{cl}$  expression,  $\gamma$  represents this damping.

This *radiation – driven* behavior affects dramatically the charged impurity scattering and eventually the conductivity. Then, first we calculate the impurity scattering rate  $W_{N,M}$  between two *oscillating* Landau states  $\Psi_N$ , and  $\Psi_M$  [32, 47, 49, 50]. Next we find the average effective distance advanced by the electron in every scattering jump:  $\Delta X^{MW} \propto A_{Lan} \cos w\tau$  [32, 39, 47], where  $\tau = 1/W_{N,M}$  is the scattering time. Finally the longitudinal conductivity  $\sigma_{xx}$  is given by:

$$\sigma_{xx} \propto \int dE \frac{\Delta X^{MW}}{\tau} \quad (3)$$

being  $E$  the energy. To obtain  $R_{xx}$  we use the relation  $R_{xx} = \frac{\sigma_{xx}}{\sigma_{xx} + \sigma_{xy}} \simeq \frac{\sigma_{xx}}{\sigma_{xy}}$ , where  $\sigma_{xy} \simeq \frac{v_i e}{B}$  and  $\sigma_{xx} \ll \sigma_{xy}$ . Therefore,

$$R_{xx} \propto \frac{eE_0}{m^* \sqrt{(w_c^2 - w^2)^2 + \gamma^4}} \cos wt = A_{Lan} \cos w\tau \quad (4)$$

and the amplitude of resistance oscillations depends linearly on the radiation electric field.

$P$  can be related with  $R_{xx}$  through the well-known formula that gives radiation intensity  $I$  (power divided by surface) in terms of the radiation electric field  $E_0$ :  $I = \frac{1}{2} c \epsilon_0 E_0^2$ , where  $c$  is the speed of light in vacuum and  $\epsilon_0$  is the permittivity in vacuum. If we want to express only the power in terms of the radiation electric field we have to take into account the sample surface. In the particular case of GaAs if  $S$  is the sample surface, we can readily obtain:

$$P = \frac{1}{2} c_{GaAs} \epsilon_{GaAs} \epsilon_0 E_0^2 S \quad (5)$$

where  $c_{GaAs}$  is the speed of light in GaAs and  $\epsilon_{GaAs}$  is the GaAs dielectric constant. Accordingly,  $E_0 \propto \sqrt{P}$ . Then, substituting in the expression of  $A_{Lan}$ , we obtain that  $R_{xx}$  varies with  $P$  following an square root law:

$$R_{xx} \propto \frac{e\sqrt{P}}{m^* \sqrt{(w_c^2 - w^2)^2 + \gamma^4}} \cos w\tau \quad (6)$$

Thus, the  $R_{xx}$  response will grow as the square root of  $P$ , i.e.,  $A \propto P^{0.5}$ . From the expression of  $R_{xx}$  we can study the influence of  $w$  and  $T$  on the sublinear relation. In the case of  $w$ , the calculation is straightforward

(see expressions of  $R_{xx}$  or  $A_{Lan}$ ). In the case of  $T$ , we introduce a microscopic model, which allow us to obtain the damping parameter  $\gamma$  and its dependence on  $T$  [32, 33, 50]. According to the model,  $\gamma$  is proportional to the scattering rate of electron-acoustic phonon interaction, being eventually linear with  $T$  [50].

## EXPERIMENTAL SET UP AND RESULTS

Low frequency lock-in based electrical measurements were carried out at  $T \leq 1.5K$  with the samples immersed in pumped liquid-helium and mounted near the open end of a microwave waveguide. [4, 13] The W (Wegscheider)-GaAs/AlGaAs single heterostructures were nominally characterized by an electron density,  $n = 2.4 \times 10^{11} cm^{-2}$  and a mobility of  $\mu = 10^7 cm^2/Vs$ . Results are reported here for measurements on a set of three W-specimens.

To examine the growth of the radiation-induced oscillations with  $P$ , Fig. 1 presents the  $\Delta R_{xx}$  of specimen W1 for several  $P$  at  $50GHz$ . Also shown in the figure are data-fits to  $\Delta R_{xx}^{fit} = -A \exp(-\lambda/B) \sin(2\pi F/B)$ . Here, a slowly varying background, approximately equaling the dark trace, was removed from the photo-excited  $R_{xx}$  data to realize  $\Delta R_{xx}$ . [29] Although this fit function includes three parameters,  $A$ ,  $\lambda$ , and  $F$ , the oscillation period in  $B^{-1}$  is independent of the radiation-intensity, and thus,  $F$  is a constant. Further, the damping constant,  $\lambda$ , [9] turns out to be insensitive to  $P$ , see Fig. 1(b). Thus, the main free parameter in the fit-function is the amplitude,  $A$ , of the oscillations. In Fig. 1(c), we exhibit the fit extracted  $A$  vs.  $P$  for W1 and W2. The figure shows a sub-linear growth of  $A$  with  $P$ . Also shown are power law fits,  $A = A_0 P^\alpha$ . Here,  $\alpha = 0.63$  and  $\alpha = 0.64$  for W1 and W2, respectively, at  $1.5K$  and  $50GHz$ .  $A_0$  varies between W1 and W2 because the effective intensity attenuation factor varies between the two experiments.

For a third W-specimen labeled W3, Fig. 1(d) and 1(e) report the influence of the temperature on the growth of  $A$  vs.  $P$ , where  $A$  is extracted, as before, from line-shape fits of the oscillatory data to  $\Delta R_{xx}^{fit} = -A \exp(-\lambda/B) \sin(2\pi F/B)$ . Here, Fig. 1(d) and 1(e) indicate that, as expected, at a constant  $P$ ,  $A$  grows with decreasing  $T$  both at  $f = 50GHz$  [Fig. 1(d)] and  $f = 46GHz$  [Fig 1(e)]. Further, the figures show that the  $A$  vs.  $P$  curves exhibit greater curvature at lower temperatures. The  $A$  vs.  $P$  have been fit once again to  $A = A_0 P^\alpha$ ; the fit-extracted  $\alpha$  and  $A_0$  have been summarized in tabular form within Fig. 1(d) and Fig. 1(e). These fit-extracted  $\alpha$  have also been plotted vs.  $T$  in the inset to these figures. These insets suggest that  $\alpha$  decreases with decreasing temperatures, consistent with the observed increased non-linearity at lower temperatures. Note that, at  $f = 50GHz$ , all three W-specimens, exhibit the same  $\alpha$ , within uncertainties, at the lowest pumped  $^4He$  temperatures. In addition, a comparison

of the  $\alpha$  reported in Fig. 1(d) and Fig. 1(e) also suggests that reducing the microwave frequency  $f$  at a fixed  $T$  tends to reduce the  $\alpha$ , i.e., increase the non-linearity. Thus, the experimental results presented here suggest a nonlinear power law in a regime characterized by moderate excitation. This peculiar behavior can be theoretically explained and the experimental results recovered by means of the radiation-driven electron orbits model. Next we present the calculated results that seem to reasonably agree with the present experiments.

## CALCULATED RESULTS

Fig. 2 presents the calculated  $R_{xx}$  as a function of  $B$  over  $0 \leq P \leq 3.7mW$  at  $f = 50GHz$  and  $T = 1K$ . As in experiments, we obtain multiple oscillations for all  $P$  except, as expected, for  $P = 0$ . It is clear the progressive collapse of  $R_{xx}$  oscillations as  $P$  decreases. The explanation is straightforward according to our theory and it is given by the expression of  $R_{xx}$ . Thus, for a decreasing (increasing)  $P$  the  $R_{xx}$  response is progressively smaller (larger). The key issue here, and the challenge for the different available theories, is to deduce the rate of increase (decrease) of  $R_{xx}$  oscillations for increasing (decreasing)  $P$ . This is shown in the inset of Fig. 2, where we present the calculated amplitude versus  $P$ . As in experiments, we obtain a clear sublinear growth of  $A$  with  $P$ :  $A \propto P^\alpha$ . We would expect an exponent  $\alpha$  around 0.5 since the model establishes an square root dependence. Thus, we have performed a fit of the calculated values, obtaining  $A = 1.66P^{0.55}$ , very close to a square root law.

The dependence of the sublinear law on  $T$  and frequency is presented in Fig. 3. In Fig. 3a we represent the calculated amplitude  $A$  of the main  $R_{xx}$  peak versus  $P$  for a frequency of  $50GHz$  and  $T$  values:  $T = 0.75K$ ,  $1.0K$ ,  $1.5K$  and  $2.0K$ . We obtain a qualitatively similar behavior as in experiments. Thus, we observe that for a constant  $P$ ,  $A$  increases (decreases) with decreasing (increasing)  $T$ . The physical explanation is as follows. If one increases  $T$ , the interaction between electrons and lattice ions also increases giving rise to a more intense damping. This implies progressively smaller amplitudes and  $R_{xx}$  oscillations tend to vanish. On the other hand, it is very clear that for all  $T$  used in the calculation, the dependence between  $A$  and  $P$  is sub-linear and that, at least qualitatively, the curves show a bigger curvature for decreasing  $T$ . To check this curvature, we have made a fit to the calculated values for each  $T$  observing that the exponent of the fits slightly increases for increasing  $T$ . In all cases, the exponent is always close to 0.5. This outcome is expected since, strictly speaking, our model does not predict any variation of the exponent with  $T$ ; our theoretical framework imposes a square root relation. Yet, experimental results show a much faster increase of the exponent with increasing  $T$  regarding the calculated

ones. The latter show a much slower variation with  $T$ , although in the same direction. At present, this model can not explain this quantitative discrepancy of the variation of  $\alpha$  with  $T$ . This discrepancy could be the result of an statistical effect of the fit or the reflex of a real physical process. In the latter case, this would imply an extension of the current theory that should start from the square root law obtained here. We consider that the square root dependence is a solid result reflecting a reasonably good agreement between theory and experiments at low temperatures.

A similar behavior is presented in Fig. 3b where we show the calculated values of  $A$  versus  $P$  for different frequencies. We observe that, as in experiments,  $A$  decreases as the frequency increases. The explanation comes from the expression of  $R_{xx}$  where  $w$  shows up in the denominator. Then, for a constant  $P$ , a larger  $w$  gives rise to smaller amplitudes. We have fit these curves and, as expected, the exponent of the fit slightly increases for increasing frequency whereas the pre-factor decreases. Yet, experiments show a much faster increase. This discrepancy is similar to the case of the  $T$ -dependence. Thus, the explanation given in Fig. 3a, applies identically here too.

All calculated results presented in Figs. 2 and 3, have been obtained directly through equation (6).

## CONCLUSIONS

In summary, experimental results indicate a nonlinear growth in the amplitude  $A$  of radiation-induced magnetoresistance oscillations with  $P$ . These results can be explained with the radiation-driven electron orbits model. According to this model, the amplitude of the radiation-induced oscillations should be proportional to the square root of radiation power, which implies a sub-linear relation. We have also studied how this sub-linear law varies with lattice temperature and radiation frequency obtaining only a qualitative good agreement between theory and experiments. The obtained quantitative discrepancies can not be explained by our theory. The origin of them could be an statistical effect or a real physical effect. In the latter case, this would imply an extension of the present theoretical model, always starting from the square root law here obtained.

R.G.M. is supported by the Army Research Office under W911NF-07-01-0158, and the Department of Energy under DOE-DE-SC-0001762. J.I. is supported by the MCYT (Spain) under grant: MAT2008-02626/NAN.

---

[1] M. Tinkham, Introduction to Superconductivity, 2nd. ed. (McGraw-Hill, New York, 1996).

- [2] R. E. Prange and S. M. Girvin, *The Quantum Hall Effect*, 2nd. ed. (Springer, New York, 1990).
- [3] S. Das Sarma and A. Pinczuk, *Perspectives in Quantum Hall Effects* (Wiley, New York, 1996).
- [4] R. G. Mani, J. H. Smet, K. von Klitzing, V. Narayanamurti, W. B. Johnson, and V. Umansky, *Nature(London)* **420**, 646 (2002).
- [5] M. A. Zudov et al., *Phys. Rev. Lett.* **90**, 046807 (2003); *Phys. Rev. B* **64**, 203111 (2001).
- [6] S. I. Dorozhkin, *JETP Lett.* **77**, 577 (2003).
- [7] R. G. Mani, V. Narayanamurti, K. von Klitzing, J. H. Smet, W. B. Johnson, and V. Umansky, *Phys. Rev.* **B69**, 161306 (2004); *Phys. Rev.* **B70**, 155310 (2004).
- [8] R. G. Mani et al., *Phys. Rev. Lett.* **92**, 146801 (2004).
- [9] R. G. Mani et al., *Phys. Rev.* **B69**, 193304 (2004).
- [10] S. A. Studenikin et al., *Sol. St. Comm.* **129**, 341 (2004).
- [11] I. V. Kukushkin et al., *Phys. Rev. Lett.* **92**, 236803 (2004).
- [12] R. L. Willett, L. N. Pfeiffer, and K. W. West, *Phys. Rev. Lett.* **93**, 026604 (2004).
- [13] R. G. Mani, *Physica E (Amsterdam)* **22**, 1 (2004); *ibid.* **25**, 189 (2004).
- [14] R. G. Mani, *Appl. Phys. Lett.* **85**, 4962 (2004); *IEEE Trans. on Nanotech.* **4**, 27 (2005); *Phys. Rev. B* **72**, 075327 (2005); *Appl. Phys. Lett.* **91**, 132103 (2007); *Sol. St. Comm.* **144**, 409 (2007); *Appl. Phys. Lett.* **92**, 102107 (2008); *Physica E*, **40**, 1178 (2008).
- [15] B. Simovic et al., *Phys. Rev.* **B71**, 233303 (2005).
- [16] J. H. Smet et al., *Phys. Rev. Lett.* **95**, 118604 (2005).
- [17] Z. Q. Yuan et al., *Phys. Rev.* **B74**, 075313 (2006).
- [18] S. A. Studenikin et al., *Phys. Rev.* **B76**, 165321 (2007).
- [19] K. Stone et al., *Phys. Rev.* **B76**, 153306 (2007).
- [20] A. Wirthmann et al., *Phys. Rev.* **B76**, 195315 (2007).
- [21] S. I. Dorozhkin et al., *Phys. Rev. Lett.* **102**, 036602 (2009).
- [22] A. T. Hatke et al., *Phys. Rev. Lett.* **102**, 086808 (2009).
- [23] R. G. Mani et al., *Phys. Rev.* **B79**, 205320 (2009).
- [24] A. C. Durst et al., *Phys. Rev. Lett.* **91**, 086803 (2003).
- [25] A. V. Andreev et al., *Phys. Rev. Lett.* **91**, 056803 (2003).
- [26] V. Ryzhii and A. Satou, *J. Phys. Soc. Jpn.* **72**, 2718 (2003).
- [27] X. L. Lei and S. Y. Liu, *Phys. Rev. Lett.* **91**, 226805 (2003).
- [28] J. Inarrea and G. Platero, *Phys. Rev. Lett.* **94**, 016806 (2005).
- [29] P. H. Rivera and P. A. Schulz, *Phys. Rev.* **B70**, 075314 (2004).
- [30] S. A. Mikhailov, *Phys. Rev.* **B70**, 165311 (2004).
- [31] I. A. Dmitriev et al., *Phys. Rev.* **B71**, 115316 (2005).
- [32] J. Iñarrea et al., *Semicond. Sci. Tech.* **9**, 515, (1994); *Phys. Rev. B*, **51**, 5244, (1995); J. Iñarrea and G. Platero *Europhys. Lett.* **34**, 43, (1996); *ibid.* **40**, 417, (1997).
- [33] J. Iñarrea and G. Platero, *Phys. Rev. B* **72** 193414 (2005); J. Iñarrea and G. Platero, *Appl. Phys. Lett.*, **89**, 052109, (2006)
- [34] A. Auerbach et al., *Phys. Rev. Lett.* **94**, 196801 (2005).
- [35] X. L. Lei and S. Y. Liu, *Phys. Rev.* **B72**, 075345 (2005).
- [36] A. D. Chepelianskii et al., *Eur. Phys. J.* **B60**, 225 (2007).
- [37] A. Auerbach and G. V. Pai, *Phys. Rev.* **B76**, 205318 (2007).
- [38] I. A. Dmitriev et al., *Phys. Rev.* **B75**, 245320 (2007).
- [39] J. Inarrea and G. Platero, *Phys. Rev.* **B78**, 193310 (2008); J. Iñarrea and G. Platero, *Appl. Phys Lett.* **89**, 172114, (2006); J. Iñarrea, *Appl. Phys Lett.* **92**, 192113,(2008)
- [40] M. Khodas and M. Vavilov, *Phys. Rev.* **B78**, 245319 (2009).
- [41] I. Finkler and B. I. Halperin, *Phys. Rev.* **B79**, 085315 (2009).
- [42] A. D. Chepelianskii and D. L. Shepelyansky, arxiv:0905.0593v1
- [43] D. Konstantinov and K. Kono, *Phys. Rev. Lett.*, **103**, 266808, (2009).
- [44] R. G. Mani et al., *Phys. Rev. B*, **81**, 125320,(2010).
- [45] J. Iñarrea and G. Platero, *Phys. Rev. B*, **76**, 073311, (2007); J. Iñarrea, *Appl. Phys. Lett.* **90**, 172118, (2007); *ibid.* **90**, 262101, (2007).
- [46] J. Iñarrea and G. Platero, *Appl. Phys Lett.* **93**, 062104, (2008).
- [47] E.H. Kerner, *Can. J. Phys.* **36**, (3) 371-377 (1958)
- [48] B.K. Ridley. *Quantum Processes in Semiconductors*, 4th ed. Oxford University Press, New York (1993).
- [49] Jesus Inarrea and Gloria Platero, *Appl. Phys. Lett.* **95**, 162106, (2009).
- [50] T. Ando, A. Fowler and F. Stern, *Rev. Mod. Phys.*, **54**, 2, p. 514, (1982).

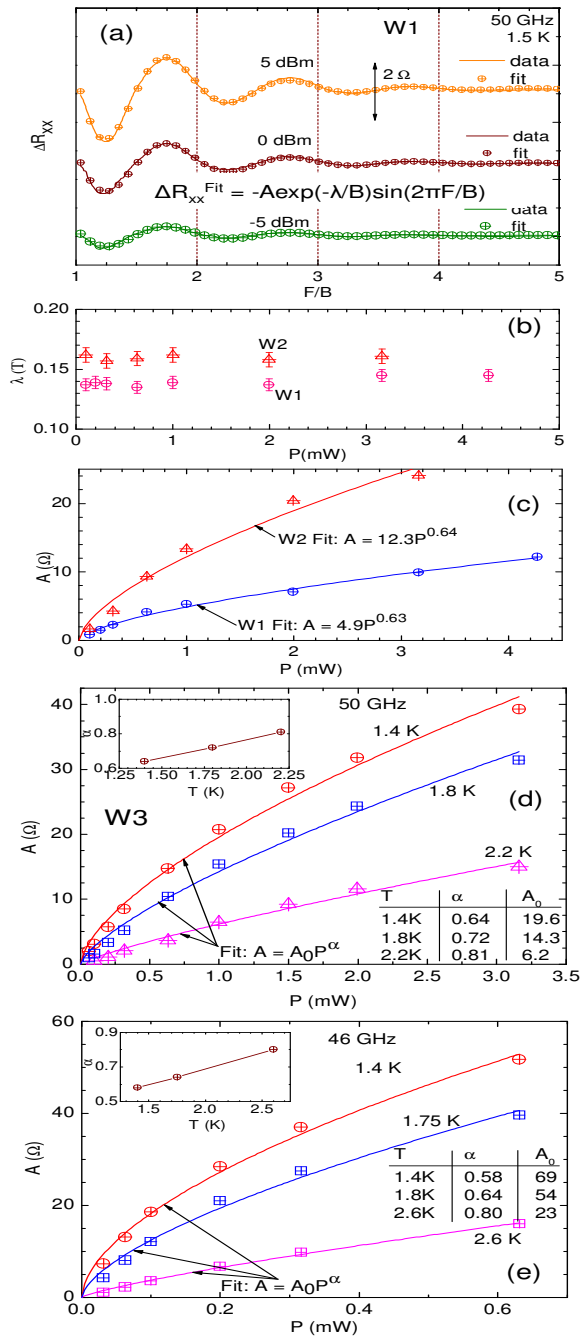


FIG. 1: (a) For W1,  $\Delta R_{xx}$  is exhibited at  $f = 50 \text{ GHz}$ . Also shown are fits to an exponentially damped sinusoid. (b)  $\lambda$  is plotted vs.  $P$  for W1 and W2. (c) The lineshape amplitude,  $A$ , is plotted vs.  $P$  for W1 and W2. Also shown are fits,  $A = A_0 P^\alpha$ , which suggest  $\alpha = 0.63$  and  $\alpha = 0.64$  for W1 and W2, respectively. (d) At  $f = 50 \text{ GHz}$ , the amplitude,  $A$ , is plotted vs.  $P$  for  $T = 1.4 \text{ K}$ ,  $1.8 \text{ K}$  and  $2.2 \text{ K}$  for W3. Also shown are fits to  $A = A_0 P^\alpha$ . The fit-extracted  $\alpha$  and  $A_0$  are presented in tabular form within the figure. The inset shows the variation of  $\alpha$  with  $T$  at  $50 \text{ GHz}$ . (e) At  $f = 46 \text{ GHz}$ , the amplitude,  $A$ , is plotted vs.  $P$  for  $T = 1.4 \text{ K}$ ,  $1.75 \text{ K}$  and  $2.6 \text{ K}$  for W3. The inset shows the variation of  $\alpha$  with  $T$  at  $46 \text{ GHz}$ .

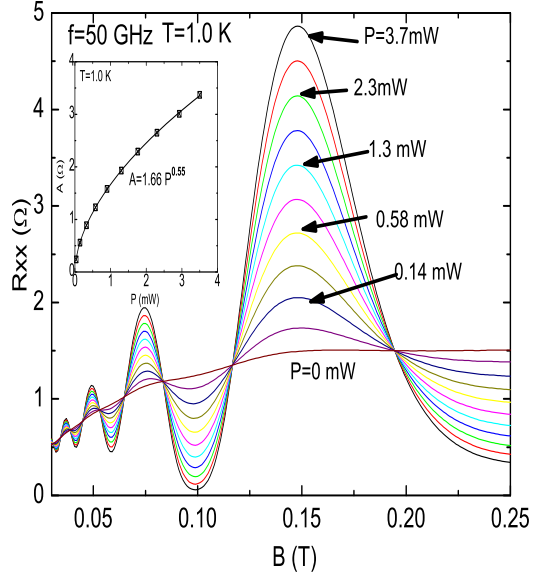


FIG. 2: Calculated  $R_{xx}$  vs.  $B$  at  $f = 50\text{GHz}$ ,  $T = 1\text{K}$ , and  $0 \leq P \leq 3.7\text{mW}$ . We obtain a progressive quenching of  $R_{xx}$  oscillations with decreasing  $P$ , leading into the dark curve ( $P = 0\text{mW}$ ). The inset shows the calculated amplitude of the main  $R_{xx}$  peak of Fig. 2 ( $B = 0.15\text{T}$ ) versus  $P$ .  $A$  increases sub-linearly with  $P$ . The line corresponds to a fit of the calculated values with  $A = 1.66P^{0.55}$  which, as expected, is very close to a square root law.

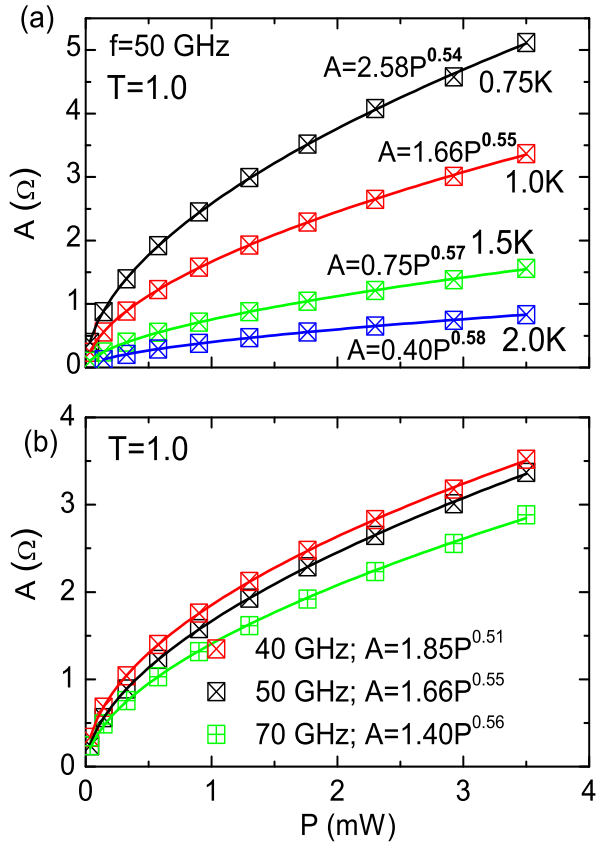


FIG. 3: (a) Calculated amplitude  $A$  of the main  $R_{xx}$  peak versus  $P$  for  $f = 50GHz$  and the  $T$  values:  $T = 0.75K$ ,  $1.0K$ ,  $1.5K$  and  $2.0K$ . Note that the dependence between  $A$  and  $P$  is sub-linear for all  $T$ . Also shown are the fits performed for each  $T$ . Observe that for increasing  $T$ , the exponent of the fit increases as the pre-factor decreases. (b) Calculated  $A$  versus  $P$  for radiation frequencies,  $40GHz$ ,  $50GHz$  and  $70GHz$  and  $T = 1K$ . We observe that  $A$  decreases as  $f$  gets larger. A fit of the  $A$  vs.  $P$  curves indicates that the exponent increases with increasing frequency, whereas the pre-factor decreases.